Materials & Design

Volume 130, 15 September 2017, Pages 1-7

Rapid spark plasma sintering to produce dense UHTCs reinforced with undamaged carbon fibres

L. Zoli [a], A. Vinci [a], L. Silvestroni [a], D. Sciti [a], M. Reece [b], S. Grasso [b]

https://doi.org/10.1016/j.matdes.2017.05.029

Highlights

- Spark plasma sintering is an efficient technique for densification of C_f - reinforced ZrB_2 materials.
- Suitable processing conditions (1800 °C/300 s/60 MPa) minimize reaction at the interface.
- Controlled fibre/matrix reaction enables fibre pull-out and non-brittle fracture.
- Uncontrolled heating leads to sample degeneration due to eutectic melting.

Abstract

Short fibre reinforced ceramic composites, based on ZrB_2 with a carbon fibre content of 45 vol%, were produced by ball-milling and rapid Spark Plasma Sintering (SPS) at 1800–2300 °C by varying the holding times. Careful control of the sintering parameters, such as the heating rate, dwell temperature and holding time are required to produce a fully dense matrix and avoid fibre degradation. The sintered materials were characterized in terms of relative density, morphology of the fibres and microstructural features of the matrix. The final residual porosity ranged from 16 to 3 vol%. The carbon fibres maintained their original morphology and the matrix consisted of ZrB_2, SiC and ZrC phases. In spite of the good adhesion between the fibre surface and the matrix promoted by SPS processing, extensive fibre pull-out was observed in the fracture surfaces of all of the composites sintered at or below 1900 °C.

Graphical abstract

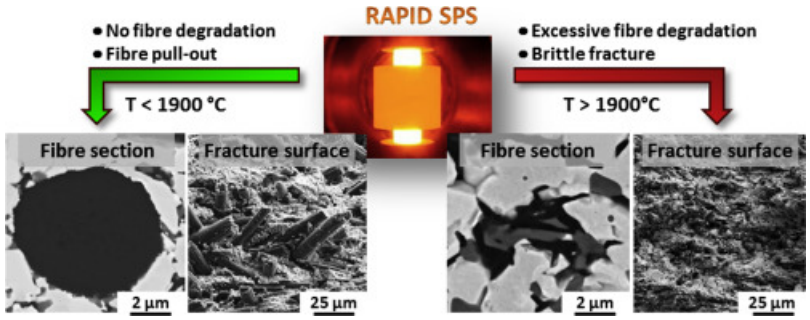

Download high-res image (327KB) Download full-size image

Keywords

Aerospace; Ceramic matrix composites; Spark plasma sintering; Eutectic temperature; ZrB_2; C

1. Introduction

Ceramic matrix composites (CMCs), such as C/C and C/SiC composites, are the materials currently used in aerospace applications for the production of thermal protection systems, leading edges and aero-engine parts [1]. The maximum working temperature of SiC-based composites is at least up to 1600 °C in an oxygen-rich atmosphere, or up to 1800 °C in low-oxygen atmosphere, due to its decomposition [2]. Recently, several research groups have proposed to integrate C or SiC fibres into a matrix consisting of ultra-high temperature ceramics (UHTCs) [3]; [4]; [5]; [6]; [7] such as borides and carbides of early transition metals, e.g. ZrB_2[8]. The resulting fibre reinforced materials can be defined as UHTCMCs [9]; [10]. Carbon and ZrB_2 are commonly employed in applications requiring extremely high temperature resistance (> 3000 °C) and excellent refractoriness in non-oxidising environments. Among the two, only ZrB_2-based composites show outstanding ablation-resistance features and good protection against oxidation at T > 1600 °C [9]; [11]; [12]; [13]; [14]. As a matter of fact, the combination of rapid heating/cooling cycles, severe thermal shock, temperatures over 1600 °C and harsh

environments is beyond the performance of current commercial materials [15]. Many approaches have been investigated to manufacture continuous carbon fibre reinforced ceramic composites, such as chemical vapour infiltration (CVI) [16], polymer infiltration and pyrolysis (PIP) [17]; [18]; [19] slurry infiltration [9] and reactive melt infiltration (RMI) [20]; [21] or a combination of these techniques. On the other hand, continuous fibre reinforced materials are anisotropic and remain expensive to manufacture. The wet/dry mixing of chopped fibres and ceramic powders offers a low cost and time-saving approach to incorporate reinforcing fibres into a UHTC matrix to avoid brittle fracture and catastrophic failure of the material [12]; [22]. However, this process poses many challenges when the amount of fibres increases to 40 vol% or more, which is desirable in order to obtain a significant decrease in weight and increased thermal shock resistance. The main issues are:

a) Achieving a homogeneous distribution of randomly oriented fibres in the UHTC matrix despite their high aspect ratio.

b) Obtaining fully dense materials while limiting fibre/matrix reaction in order to achieve a weak interface. This is an essential requirement to achieve a non-brittle failure mode, typical of CMCs.

Incorporation of large amounts of fibres (45 vol%) was found to be feasible in our previous work using conventional powder metallurgy methods and hot pressing [12]. Remarkably, other authors successfully tested alternative processes based on sol-gel techniques and this approach minimized the fibre damage (20 vol%) [23]; [24].

Achieving densities higher than 90% with a fibre content > 40 vol% is not trivial. In our previous work [12], the maximum relative density was around 85% (C_f = 45 vol%) for analogue composites hot pressed at 1800 °C with 30 MPa of applied pressure. As for the fibre/matrix interface, in a previous work, composites with 10 and 20 vol% of carbon fibres were manufactured to study the C/ZrB_2 interface and it was found that the extent of damage induced by processing depends on many factors, including the fibre type (pan or pitch derived), the use of sintering aid and sintering temperature [25]. Based on previous experience [26], Si_3N_4 was selected as sintering aid, while SiC was added to improve oxidation resistance of the ZrB_2 matrix: [26]. Therefore, we selected 1800 °C as starting reference temperature and subsequently increased both temperature and pressure to reduce the residual porosity upon rapid spark plasma sintering (SPS) tests.

In the present work, the possibility to achieve nearly fully dense UHTCMCs by the rapid SPS technique, while preserving the fibres integrity, was investigated. Spark plasma sintering is a well-established consolidation technique that can pomote near full densification of ceramics in short processing times of the order of minutes. This is especially true for conductive ceramics, such as borides and carbides, where the electrical currents have been demonstrated to significantly enhance densification by eliminating oxide phases like M_xO_y and B_2O_3[27]. The inherent advantages of SPS processing are the rapid heating rate, which is up to 1000 °C/min in the case of rapid SPS [28]; [29]; [30] and up to 10,000 °C/min for Flash SPS technique [31]. Such high heating rates, besides contributing to a significant energy saving during the consolidation process, also enable the possibility to produce metastable materials, which would not be possible to achieve using other sintering routes.

The production and microstructure evolution of ZrB_2 + 8 vol% Si_3N_4 + 3 vol% SiC, materials reinforced with 45 vol% of high modulus pitch based chopped fibres is presented and correlated to the sintering temperature and time.

2. Experimental

For the fabrication of the ceramic composites, the following raw materials were used: ZrB_2 (Grade B, H.C. Starck, Germany), specific surface area 1.0 m^2/g, particle size range 0.5–6 μm, impurities (wt%): 0.25 C, 2.00 O, 0.25 N, 0.10 Fe, 0.20 Hf; α-SiC (Grade UF-25, H.C. Starck, Germany) specific surface area 23–26 m^2/g, D_{50} 0.45 μm; Si_3N_4 (Baysinid Bayer, Germany), specific surface area 12.2 m^2/g, mean particle size 0.15 μm, impurities (wt%): 1.5 O; commercial in-house chopped high modulus pitch-derived C_f with diameter 7–10 μm and chopped length: 1 mm.

The fibres and ceramic powders mixture, 55 vol% (89 vol% ZrB_2 + 8 vol% Si_3N_4 + 3 vol% SiC) + 45 vol% C_f, was prepared by wet ball-milling, drying and sieving according to [12]. A series of green pellets (ϕ = 20.5 mm, h = 6 mm, m = 5.6 g) was obtained by compacting the C_f-ZrB_2-SiC mixture into a 20.5 mm diameter steel die with an hydraulic press at 60 MPa.

In a typical sintering experiment, the pressed pellet was inserted into a hollow graphite die with 20.5 mm inner diameter. All the experiments were carried out using an SPS furnace (FCT HPD 25; FCT Systeme GmbH, Rauenstein, Germany) under vacuum (5 Pa). The temperature probed by a top pyrometer was increased from 450 to 1400 °C in 5 min (190 °C/min) under a constant pressure of 16 MPa. The sample was maintained at 1400 °C for 5 min while the pressure was linearly increased to 60 MPa. During this step, the temperature within the die homogenised and some of the gases produced escaped through the open porosity. In order to minimize the thermal degradation of the carbon fibres, we used a rapid heating of 1000 °C/min up to the sintering temperature. The SPS sintering was carried out first at 1800 °C, increasing the holding time until no further shrinkage was observed; additionally two other sintering cycles were carried out at 1850 °C and 1900 °C. All the experiments were performed applying a pressure of 60 MPa (see sample A–E, Table 1). The heating time was controlled using a unit of second. Finally, one experiment was carried out at a much higher heating rate of about 3000 °C/min, close to the FSPS regime [31], with the purpose of studying the effect of ultra-rapid heating on the microstructure of C_f/ZrB_2 system (sample **F**, Table 1). The set cooling rate was for all samples 500 °C/min.

Table 1. Sintering cycles, densities and porosities of the ZrB_2 – C_f composites.

Label	Actual ramp[a] (°C/min)	Temperature (°C)	Holding time (sec)	Bulk density (g/cm^3)	Porosity (%)	ZrB_2 grain size (μm)
A	1043	1800	44	3.46	16.5	2.27
B	1043	1800	90	3.78	9.3	2.45
C	1043	1800	300[b]	3.83	8.3	2.38
D	1080	1850	180[b]	3.98	4.5	2.42
E	1200	1900	60[b]	4.03	3.3	2.46
F	> 3000[c]	> 2000[c]	30	4.15	< 1.0	2.59

The temperature was probed by a top pyrometer pointed on a graphite punch 4 mm from the sample.

a
The furnace power is set in order to achieve a heating rate of 1000 °C/min, minor fluctuations are seen due to the PID (proportional–integral–derivative) controllers operated at very high heating rates.

b
The sintering cycles end when no further shrinkage is observed.

c
The exact heating rate and temperature are unknown due to the extremely high power applied.

The theoretical density of the materials, based on the initial composition, was calculated using the rule of mixtures. The bulk density of the sintered pellets was determined using Archimedes' method, while the relative density, ρ, was defined as the ratio between the experimental and the theoretical values; finally, the residual porosity volume fraction was derived as (1-ρ)· 100.

The microstructures were analysed on polished and fractured surfaces using field emission scanning electron microscopy (FE-SEM, Carl Zeiss Sigma NTS Gmbh Öberkochen, Germany) and energy dispersive X-ray spectroscopy (EDS, INCA Energy 300, Oxford instruments, UK).

The average grain size and maximum fibre length were measured by image analysis (Image-Pro analizer 7.0) carried out onto SEM micrographs of polished sintered sections.

To obtain an insight into the fracture mode of the various specimens, four point bending strength tests were carried out on selected samples. The test bars, 20 × 2.5 × 2 mm^3 (length by width by thickness, respectively), were machined from the sintered pellets using diamond tool machining and fractured using a semi-articulated stainless steel four-point fixture with a lower span of 16 mm and an upper span of 8 mm using a screw-driven load frame (Instron mod. 6025, Instron, High Wycombe, GB).

3. Results and discussion

The bulk density and the residual porosity of the composites are reported in Table 1. The lowest relative density of 84% was obtained for the sample sintered at 1800 °C for a dwell time of 40 s (**A**). When the dwell time was extended to 90 s (**B**), a densification degree higher than 90% was achieved. An increase in the sintering temperature from 1800 °C to 1850 °C led to a decrease of the porosity from 8.3% (**C**) to 4.5% (**D**); a further increase of the sintering temperature to 1900 °C did not have any major effects on densification (**E**). When a heating rate of ~ 3000 °C/min was used, like in flash SPS [31], extreme damage of the carbon fibres was observed (**F**), as illustrated later. This suggests that in order to achieve dense samples while preserving the fibres structural and morphological integrity, precise temperature control is needed, rather than an ultra-fast processing time, of just a few seconds.

It has to be mentioned that in the ZrB_2–SiC–C system, several eutectic temperatures exist: at 2100–2200 °C for the three-component system [32], at 2270 °C between ZrB_2-SiC [33], and at 2390 °C between ZrB_2-C [34]. These set the threshold of temperatures that should not be exceeded during processing and usage.

It is interesting to compare these results with our previous ones where we sintered a composite with 45 vol% of Carbon short fibres [12] at 1800 °C/30 MPa/10 min by hot pressing, reaching just 85% of relative density. This result is quite similar to sample **A**, which however, underwent a much shorter holding time (40 s vs 10 min). In this case both the enhanced pressure (60 MPa) and the more efficient heating (Joule heating) allowed a fast densification that was easily improved with the increase of the maximum temperature at 1850 and 1900 °C.

3.1. Microstructural analysis of UHTCMC

Polished and fractured sections of all of the samples are shown in Fig. 1 and Fig. 2, respectively. For reference, the polished section of sample **E** is also shown in Fig. 3a, while EDS analysis of the secondary phases are reported in Fig. 3b.

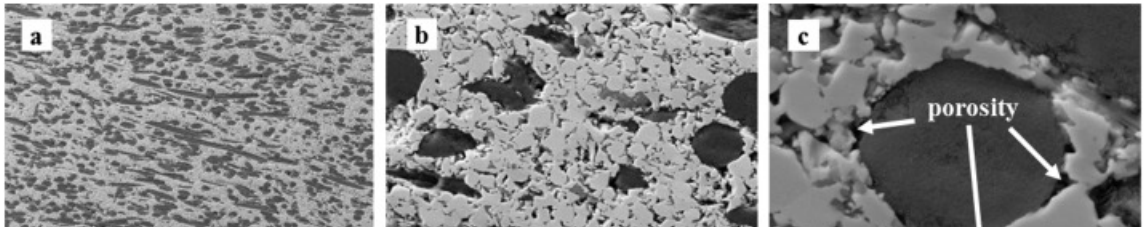

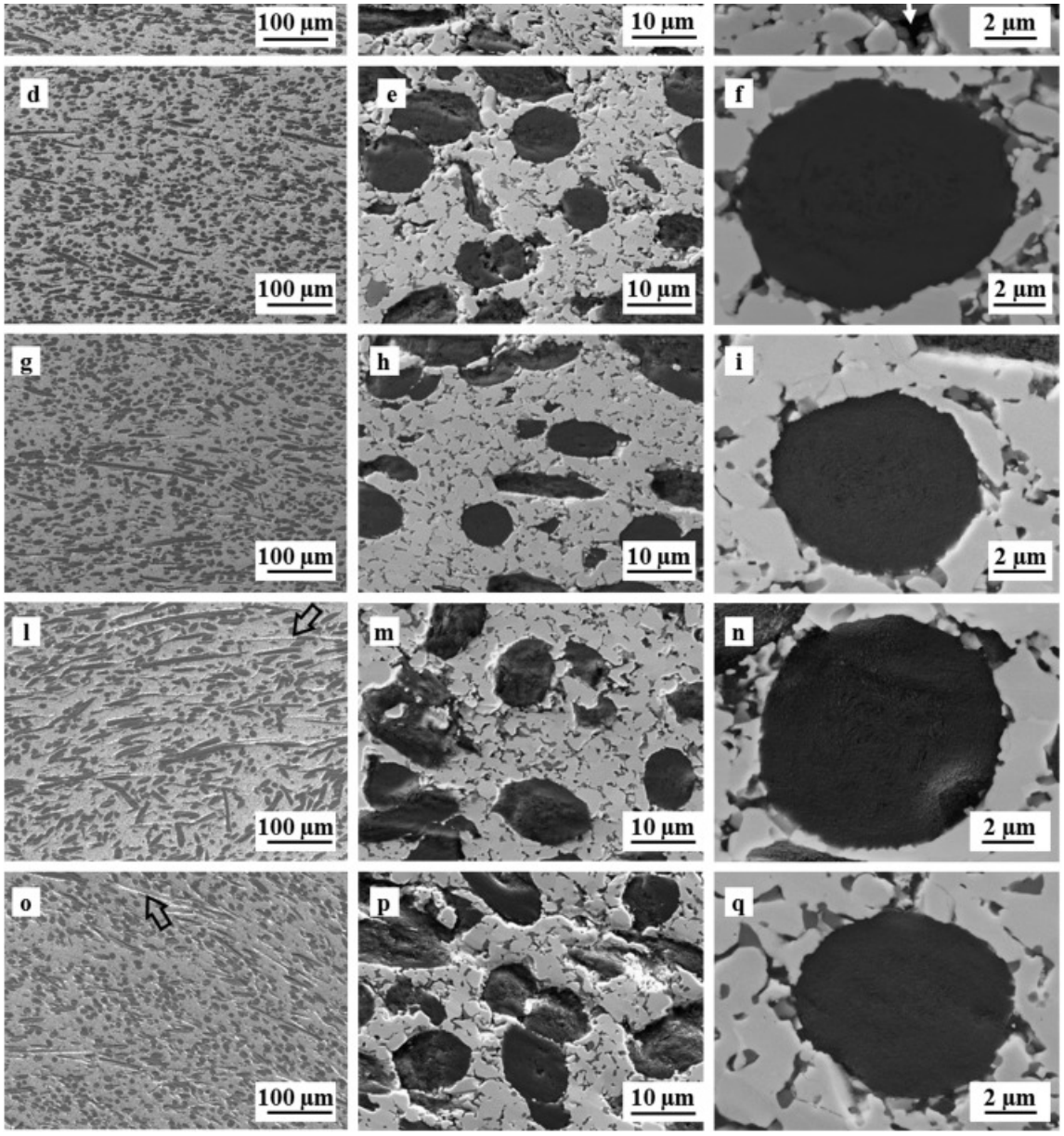

Download high-res image (2MB) Download full-size image

Fig. 1. Polished sections of samples: a–c) **A**; d–f) **B**; g–i) **C**; l–n) **D**; o–q) **E** showing the overall fibre distribution (left), a magnification of the matrix densification degree (centre) and the fibre section with secondary phases at the interface (right).

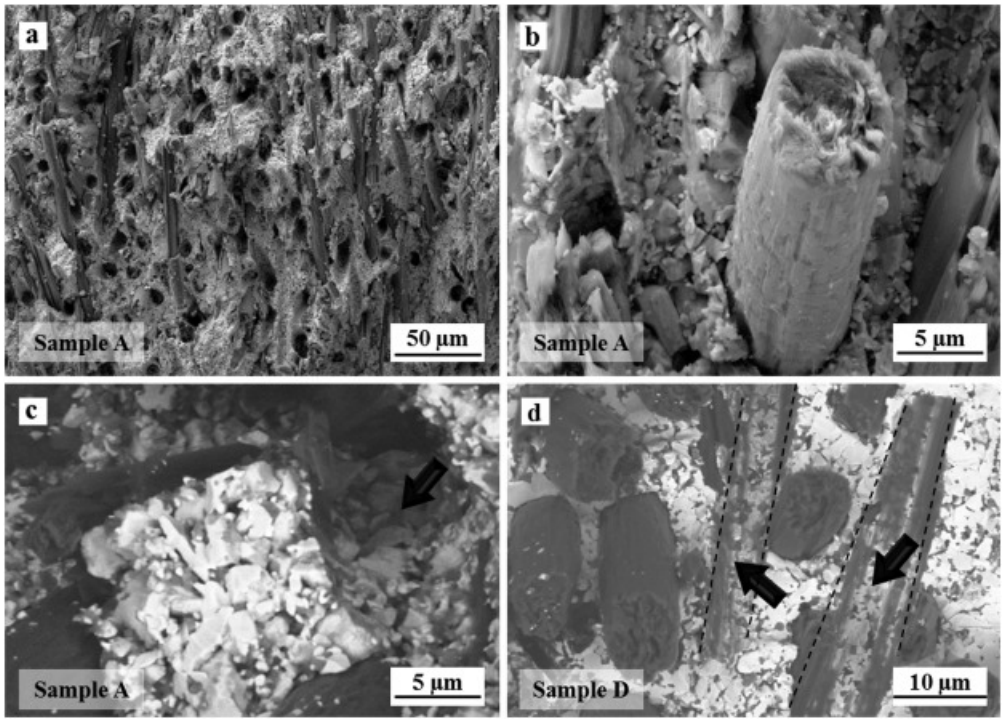

Download high-res image (1018KB) Download full-size image

Fig. 2. Fracture surfaces showing a) diffuse pull-out, b) detail of a fibre pull-out and c) pull-out without or d) with detachment of the outermost C_f layers indicated by arrows, as a consequence of a different fibre-matrix interaction.

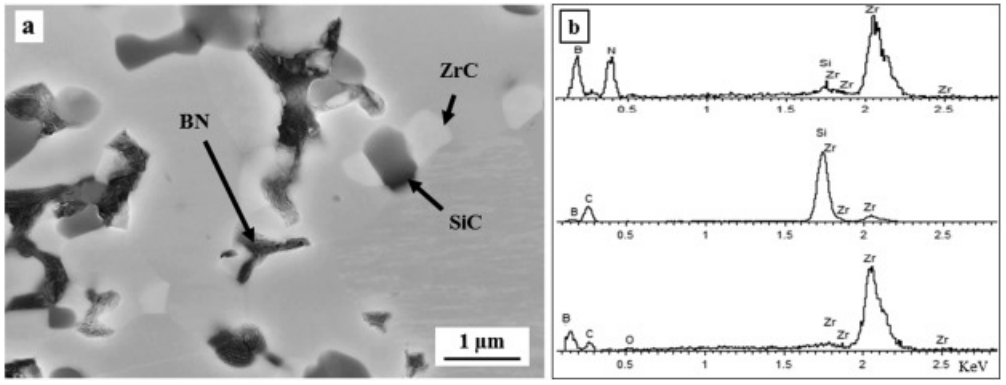

Download high-res image (261KB) Download full-size image

Fig. 3. a) Detail of the polished section of sample **E**, where arrows highlight the formed secondary phases with the corresponding EDS spectra in b).

As shown in Fig. 1a–o (left column) the dispersion of the fibres into the matrix is homogeneous for all of the samples, since no agglomeration was found. The maximum length of the fibres measured on the surface perpendicular to the pressing direction is around 300 μm, an order of magnitude lower than the starting fibres. This reduction on the size length is due to the milling process as already reported in [25]; [35]. The groove pointed by the black arrows in Fig. 1 are fibres removed during polishing. Furthermore the same images highlight that, as in our previous works [12]; [25], most of the fibres tend to align their long axis perpendicularly to the applied pressure (here defined as Z-axis) during sintering, even if they are distributed randomly along the XY axes. The preferential distribution is due both to the shaping process and the applied pressure during sintering. Fig. 1 b–p (central column) and c–q (right column) better evidence some microstructural details, such as a higher residual porosity in sample **A**, higher densities for samples **B**, **C**, **G**, **E**, and the presence of SiC based phases (grey contrast) with an average particle size of about 2 μm. As a matter of fact, XRD patterns, reported in Fig. S1 (see Supplementary material), just showed reflections belonging to the constituent phases, e.g. ZrB_2 (Zirconium diboride, #34-0423), C (Graphite-2H, #41-1487) and SiC (Moissanite-6H-syn, #29-1131). Instead, detailed SEM-EDS analyses highlighted the formation of new phases, identified as ZrC and BN, Fig. 3. Formation of these phases is not a novelty; previous SEM and TEM analyses [11]; [25]; [26]; [35] revealed that BN forms during densification of ZrB_2 when Si_3N_4 is added as sintering aid, according to:

$$Si_3N_4 + 2B_2O_3 = 3SiO_2 + 4BN \quad (1)$$

ZrC is instead formed due to reaction between ZrO_2, always coating ZrB_2 particles, and C, according to:

$$ZrO_2 + 3C = ZrC + 2CO \quad (2)$$

These phases are hardly detected by XRD due to their low amount (< 5 vol%).

The type of interaction between fibres and matrix is an important feature of composites, because crack deflection, crack bridging and fibre pull-out are ascribed as responsible for the activation of toughening mechanisms.

Comparing the fracture surfaces, fibre pull-out can be observed in all the samples, as for example in Fig. 2a. As expected, a higher degree of densification of the composite leads to a less pronounced pull-out. Compared to PAN-based fibres [25], pitch-based fibres allow an extensive pull-out from the UHTC matrix upon fracture, due to a lower tendency to react with the surrounding matrix. The reason lies in the onion-like structure of such graphitic fibres that, during crack propagation, allow the detachment of external graphite layers from the fibre core upon the establishment of the optimum fibre-matrix interface. The evidence for this behaviour is well demonstrated in the backscattered micrographs of Fig. 2c, d, where the naked “fibre-fingerprint” is visible on the matrix (*black arrow* in Fig. 2c) or presents graphite layers externally detached from the fibre (*black arrow* in Fig. 2d). This phenomenon is more visible in the near fully dense samples, **C**, **D** and **E**.

3.1.1. Eutectic temperature and fibre deterioration

A unambiguous method to evaluate the degradation degree of carbon fibre has not been assessed yet, therefore we can just speculate on the fibre integrity by SEM analysis. Another possibility could be localized mechanical testing by indentation technique. Since this procedure is quite complex, at the moment our analyses focus on the interface and inner fibre morphology, as observed by electron microscopy.

The microstructure of the polished and fractured surface of the sample sintered at a ultra-high heating rate, sample **F**, is shown in Fig. 4a and b respectively. The morphology of the fibres is no longer rounded, but rather irregular and open. Moreover, some of the carbon fibres embed ZrB_2 grains inside their layered structure and some of the grains display the typical lamellar structure of ZrB_2-SiC produced by solidification from the eutectic phase, e.g. in Fig. 4a. Such behaviour can only be explained by the sintering

temperature exceeding 2270 °C. Unfortunately, precise control of the final temperature and an estimate of the heating ramp were not possible for this sample due to the high power/heating rate applied (close to the FSPS regime).

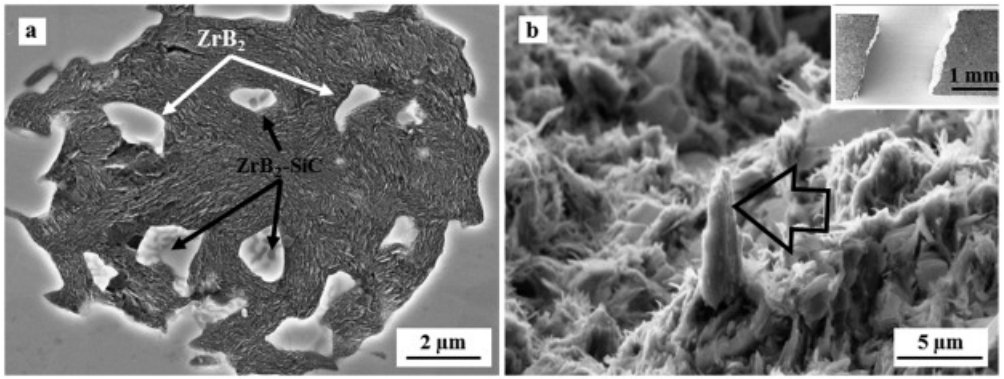

Download high-res image (569KB) Download full-size image

Fig. 4. a) Details of the polished surface of sample **F** showing the fibre shape; arrows highlight the presence of ZrB_2 or ZrB_2-SiC grains inside the fibre. b) Detail of the fracture section showing graphite spikes pulling out from the surface, due to fibre degradation (pointed by the arrow). The inset in b) shows the top view of the fractured bar upon four point bending test (sample **A–E** remained entire after fracture due to fibre bringing).

Also of note, the interpenetration of ZrB_2 grains inside the fibres in sample **F** and notable fibre damage lead to brittle fracture without fibre pull-out, with graphite spikes rising only a few μm over the ZrB_2 grains, as shown in Fig. 4b.

3.2. Mechanical behaviour

Due to the small size of the sintered samples (d = 20 mm), it was not possible to carry out a systematic investigation of the mechanical properties of the composites. However, to obtain a preliminary indication of the fracture behaviour of such short fibre reinforced ceramic composites, we performed 4-point bending tests. A comparison of typical load/displacement curves recorded for three selected samples with different levels of densification, sample **A** (RD = 84%), sample **C** (RD = 92%) and sample **E** (RD = 97%), is shown in Fig. 5a, while the lateral view of the bar after four point bending test for the sample **C** is reported at two different magnifications in Fig. 5b, c. The strength values, taken merely as indicative numbers, were in the 70–100 MPa range, similar to other previous results obtained by HP [12]. The fracture behaviour of the overheated sample **F** (not shown in Fig. 5a) has the highest absolute strength value of 200 MPa, but the bar was found broken in a brittle mode (see the inset in Fig. 4b), whilst the bars machined from samples **A**, **C**, **E** behaved in non-brittle mode due to a combination of reinforcing phenomena, such as extensive fibre bridging, fibre pull-out and crack deflection along the fracture (Fig. 5b, c). We interpreted such differences in fracture behaviour as being determined by the properties of the fibre-matrix interface. In the case of sample **A**, there was limited interaction between the partially porous matrix and the fibre, i.e. the fibre-matrix interface was too weak. On the other hand, for sample **E**, which was almost fully dense, the fibre-matrix interface is so strong to significantly reduce fibre pull-out and crack deflection. However a better densification of samples **E** and **F** led to a higher ultimate strength as compared to **A** and **C**, with a fracture behaviour typical of bulk ceramics rather than CMCs. The best compromise seems to be achieved in sample **C**, where an adequate combination of matrix density and fibre-matrix interface strength results in a failure tolerant behaviour.

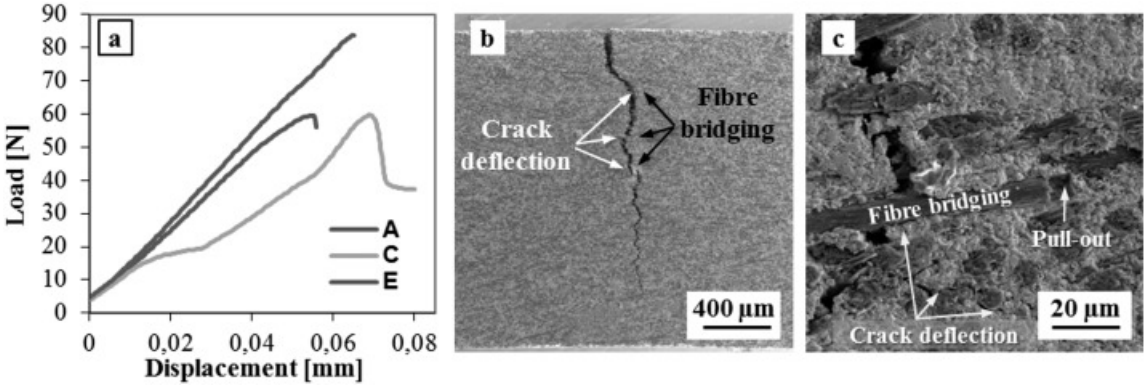

Download high-res image (471KB) Download full-size image

Fig. 5. a) Comparison of load/displacement curves for sample with different porosity level: 16% (A), 8% (C) and 3% (E); b, c) are the lateral view of the bar of sample **C** after four point bending test showing multiple reinforcing mechanisms.

One aspect that we neglected in these preliminary mechanical tests is the development of compressive-tensile stresses, due to the combination of ZrB_2 and C_f with different elastic properties and coefficients of thermal expansion mismatch, upon the achievement of a partial or full matrix density.

4. Conclusions

Spark plasma sintering processing was used to produce dense short fibre-reinforced ceramic composites based on ZrB_2 with a carbon fibres content of 45 vol%. The relative density of 96.7%, achieved for samples sintered at 1900 °C, is significantly higher than analogous specimens produced by conventional hot pressing, which achieved only 85% of the theoretical density. Careful control of the sintering parameters, such as the heating rate, maximum temperature and holding time resulted in materials with near full density and no appreciable damage of the carbon fibres.

It has also been assessed that above a critical temperature (> 1900 °C), set by the eutectic melt met in the ZrB_2-SiC-C system, extreme fibre degradation occurs, with associated brittle behaviour of the composite. It has also been observed that slight deviations in the density level have a strong impact on the fracture behaviour.

The following are the supplementary data related to this article.

Download Powerpoint document (2MB) Help with pptx files

Fig. S1. X-ray diffraction pattern recorded on the section of sample **A** where the following phases were identified: ZrB_2 (Zirconium diboride, #34-0423), C (Graphite-2H, #41-1487) and SiC (Moissanite-6H-syn, #29-1131).

Acknowledgements

Authors wish to thank G. Angeloni s.r.l. for providing carbon fibres. S.G. and M.J.R. were supported by EPSRC (EP/K008749/1, XMat).

Recommended articles Citing articles (1)

References

[1] W. Krenkel
Ceramic Matrix Composites: Fiber Reinforced Ceramics and Their Applications
Wiley-VCH Verlag GmbH & Co. KGaA, Weinheim, Germany (2008), 10.1002/9783527622412
Google Scholar

[2] M.E. Westwood, J.D. Webster, R.J. Day, F.H. Hayes, R. Taylor
Review oxidation protection for carbon fibre composites
J. Mater. Sci., 31 (1996), pp. 1389-1397, 10.1016/0008-6223(89)90204-2
CrossRef View Record in Scopus Google Scholar

[3] A.L. Chamberlain, W.G. Fahrenholtz, G.E. Hilmas, D.T. Ellerby
High-strength zirconium diboride-based ceramics
J. Am. Ceram. Soc., 87 (2004), pp. 1170-1172
(doi:Cited By (since 1996) 255\nExport Date 14 June 2012)
CrossRef View Record in Scopus Google Scholar

[4] M.M. Opeka, I.G. Talmy, E.J. Wuchina, J.A. Zaykoski, S.J. Causey
Mechanical, thermal, and oxidation properties of refractory hafnium and zirconium compounds
J. Eur. Ceram. Soc., 19 (1999), pp. 2405-2414, 10.1016/S0955-2219(99)00129-6
Article Download PDF View Record in Scopus Google Scholar

[5] S. Tang, J. Deng, S. Wang, W. Liu, K. Yang
Ablation behaviors of ultra-high temperature ceramic composites
Mater. Sci. Eng. A, 465 (2007), pp. 1-7, 10.1016/j.msea.2007.02.040
Article Download PDF CrossRef View Record in Scopus Google Scholar

[6] Q. Li, S. Dong, Z. Wang, G. Shi
Fabrication and properties of 3-D C_f/ZrB_2-ZrC-SiC composites via polymer infiltration and pyrolysis
Ceram. Int., 39 (2013), pp. 5937-5941, 10.1016/j.ceramint.2012.11.074
Article Download PDF View Record in Scopus Google Scholar

[7] B. Xu, C. Hong, S. Zhou, J. Han, X. Zhang

High-temperature erosion resistance of ZrB_2-based ceramic coating for lightweight carbon/carbon composites under simulated atmospheric re-entry conditions by high frequency plasma wind tunnel test

Ceram. Int., 42 (2016), pp. 9511-9518, 10.1016/j.ceramint.2016.03.029

Article Download PDF View Record in Scopus Google Scholar

[8] W.G. Fahrenholtz, G.E. Hilmas, I.G. Talmy, J.A. Zaykoski

Refractory diborides of zirconium and hafnium

J. Am. Ceram. Soc., 90 (2007), pp. 1347-1364, 10.1111/j.1551-2916.2007.01583.x

CrossRef View Record in Scopus Google Scholar

[9] L. Zoli, D. Sciti

Efficacy of a ZrB_2–SiC matrix in protecting C fibres from oxidation in novel UHTCMC materials

Mater. Des., 113 (2017), pp. 207-213, 10.1016/j.matdes.2016.09.104

Article Download PDF View Record in Scopus Google Scholar

[10] C.J. Leslie, E.E. Boakye, K.A. Keller, M.K. Cinibulk

Development and characterization of continuous SiC fiber-reinforced HfB_2-based UHTC matrix composites using polymer impregnation and slurry infiltration techniques

Int. J. Appl. Ceram. Technol., 12 (2015), pp. 235-244, 10.1111/ijac.12279

CrossRef View Record in Scopus Google Scholar

[11] F. Monteverde, S. Guicciardi, A. Bellosi

Advances in microstructure and mechanical properties of zirconium diboride based ceramics

Mater. Sci. Eng. A, 346 (2003), pp. 310-319, 10.1016/S0921-5093(02)00520-8

Article Download PDF View Record in Scopus Google Scholar

[12] D. Sciti, L. Zoli, L. Silvestroni, A. Cecere, G.D. Di Martino, R. Savino

Design, fabrication and high velocity oxy-fuel torch tests of a Cf-ZrB_2-fiber nozzle to evaluate its potential in rocket motors

Mater. Des., 109 (2016), pp. 709-717, 10.1016/j.matdes.2016.07.090

Article Download PDF View Record in Scopus Google Scholar

[13] E.W. Neuman, G.E. Hilmas, W.G. Fahrenholtz

Mechanical behavior of zirconium diboride-silicon carbide ceramics at elevated temperature in air

J. Eur. Ceram. Soc., 33 (2013), pp. 2889-2899, 10.1016/j.jeurceramsoc.2013.05.003

Article Download PDF View Record in Scopus Google Scholar

[14] A. Paul, J. Binner, B. Vaidhyanathan

UHTC composites for hypersonic applications

W. Fahrenholtz, E. Wuchina, W. Lee, Y. Zhou (Eds.), Ultra-high Temperature Ceramics: Materials for Extreme Environment Applications, Wiley, Inc. (2014), pp. 144-166

ISBN 0-471-9781118700785 Copyright © 2014

10.1002/9781118700853.ch7

CrossRef View Record in Scopus Google Scholar

[15] J.W. Zimmermann, G.E. Hilmas, W.G. Fahrenholtz
Thermal shock resistance of ZrB_2 and ZrB_2-30% SiC
Mater. Chem. Phys., 112 (2008), pp. 140-145, 10.1016/j.matchemphys.2008.05.048
Article Download PDF View Record in Scopus Google Scholar

[16] A. Paul, S. Venugopal, J.G.P. Binner, B. Vaidhyanathan, A.C.J. Heaton, P.M. Brown
UHTC-carbon fibre composites: preparation, oxyacetylene torch testing and characterisation
J. Eur. Ceram. Soc., 33 (2013), pp. 423-432, 10.1016/j.jeurceramsoc.2012.08.018
Article Download PDF View Record in Scopus Google Scholar

[17] H. Hu, Q. Wang, Z. Chen, C. Zhang, Y. Zhang, J. Wang
Preparation and characterization of C/SiC–ZrB_2 composites by precursor infiltration and pyrolysis process
Ceram. Int., 36 (2010), pp. 1011-1016, 10.1016/j.ceramint.2009.11.015
Article Download PDF View Record in Scopus Google Scholar

[18] C. Ma, L. Guo, H. Li, W. Tan, T. Duan, N. Liu, M. Zhang
Effects of high-temperature annealing on the microstructures and mechanical properties of C/C–ZrC–SiC composites prepared by precursor infiltration and pyrolysis
Mater. Des., 90 (2016), pp. 373-378, 10.1016/j.matdes.2015.10.140
Article Download PDF View Record in Scopus Google Scholar

[19] X. He, Y. Zhou, D. Jia, Y. Guo
Effect of sintering additives on microstructures and mechanical properties of short-carbon-fiber-reinforced SiC composites prepared by precursor pyrolysis-hot pressing
Ceram. Int., 32 (2006), pp. 929-934, 10.1016/j.ceramint.2005.07.007
Article Download PDF View Record in Scopus Google Scholar

[20] M. Kütemeyer, L. Schomer, T. Helmreich, S. Rosiwal, D. Koch
Fabrication of ultra high temperature ceramic matrix composites using a reactive melt infiltration process
J. Eur. Ceram. Soc., 36 (2016), pp. 3647-3655, 10.1016/j.jeurceramsoc.2016.04.039
Article Download PDF View Record in Scopus Google Scholar

[21] S. Chen, C. Zhang, Y. Zhang, H. Hu
Influence of pyrocarbon amount in C/C preform on the microstructure and properties of C/ZrC composites prepared via reactive melt infiltration
Mater. Des., 58 (2014), pp. 570-576, 10.1016/j.matdes.2013.12.071
Article Download PDF View Record in Scopus Google Scholar

[22] J.J. Sha, J. Li, S.H. Wang, Y.C. Wang, Z.F. Zhang, J.X. Dai
Toughening effect of short carbon fibers in the ZrB_2–$ZrSi_2$ ceramic composites
Mater. Des., 75 (2015), pp. 160-165, 10.1016/j.matdes.2015.03.006
Article Download PDF View Record in Scopus Google Scholar

[23] F. Yang, X. Zhang, J. Han, S. Du
Processing and mechanical properties of short carbon fibers toughened zirconium diboride-based ceramics

Mater. Des., 29 (2008), pp. 1817-1820, 10.1016/j.matdes.2008.03.011
Article Download PDF View Record in Scopus Google Scholar

[24] J.J. Sha, J. Li, S.H. Wang, Z.F. Zhang, Y.F. Zu, S. Flauder, W. Krenkel
Improved microstructure and fracture properties of short carbon fiber-toughened ZrB_2-based UHTC composites via colloidal process
Int. J. Refract. Met. Hard Mater., 60 (2016), pp. 68-74, 10.1016/j.ijrmhm.2016.07.010
Article Download PDF View Record in Scopus Google Scholar

[25] L. Silvestroni, D. Dalle Fabbriche, C. Melandri, D. Sciti
Relationships between carbon fiber type and interfacial domain in ZrB_2-based ceramics
J. Eur. Ceram. Soc., 36 (2016), pp. 17-24, 10.1016/j.jeurceramsoc.2015.09.026
Article Download PDF View Record in Scopus Google Scholar

[26] D. Sciti, L. Silvestroni, V. Medri, F. Monteverde
Sintering and densification of ultra-high temperature ceramics
W. Fahrenholtz, E. Wuchina, W. Lee, Y. Zhou (Eds.), Ultra-high Temperature Ceramics: Materials for Extreme Environment Applications, Wiley, Inc. (2014), pp. 112-143
ISBN 0-471-9781118700785 Copyright © 2014
10.1002/9781118700853.ch6
CrossRef View Record in Scopus Google Scholar

[27] J. Gonzalez-Julian, K. Jähnert, K. Speer, L. Liu, J. Räthel, M. Knapp, H. Ehrenberg, M. Bram, O. Guillon
Effect of internal current flow during the sintering of zirconium diboride by field assisted sintering technology
J. Am. Ceram. Soc., 99 (2016), pp. 35-42, 10.1111/jace.13931
CrossRef View Record in Scopus Google Scholar

[28] S. Grasso, C. Hu, G. Maizza, Y. Sakka
Spark plasma sintering of diamond binderless WC composites
J. Am. Ceram. Soc., 95 (2012), pp. 2423-2428, 10.1111/j.1551-2916.2011.05009.x
CrossRef View Record in Scopus Google Scholar

[29] G.B. Yadhukulakrishnan, S. Karumuri, A. Rahman, R.P. Singh, A. Kaan Kalkan, S.P. Harimkar
Spark plasma sintering of graphene reinforced zirconium diboride ultra-high temperature ceramic composites
Ceram. Int., 39 (2013), pp. 6637-6646, 10.1016/j.ceramint.2013.01.101
Article Download PDF View Record in Scopus Google Scholar

[30] E. Zapata-Solvas, D.D. Jayaseelan, H.T. Lin, P. Brown, W.E. Lee
Mechanical properties of ZrB_2- and HfB_2-based ultra-high temperature ceramics fabricated by spark plasma sintering
J. Eur. Ceram. Soc., 33 (2013), pp. 1373-1386, 10.1016/j.jeurceramsoc.2012.12.009
Article Download PDF View Record in Scopus Google Scholar

[31] S. Grasso, T. Saunders, H. Porwal, O. Cedillos-Barraza, D.D. Jayaseelan, W.E. Lee, M.J. Reece
Flash spark plasma sintering (FSPS) of pure ZrB_2

J. Am. Ceram. Soc., 97 (2014), pp. 2405-2408, 10.1111/jace.13109
CrossRef View Record in Scopus Google Scholar

[32] D.A. Krivoshein, I.A. Sobol, M.A. Maurakh, V.S. Dergunova, Y.N. Petrov
Wetting of carbon materials by the eutectic ZrB_2-Si-C alloy
Sov. Powder Metall. Met. Ceram., 19 (1980), pp. 183-185, 10.1007/BF00798476
CrossRef View Record in Scopus Google Scholar

[33] R. Tu, H. Hirayama, T. Goto
Preparation of ZrB_2-SiC composites by arc melting and their properties
J. Ceram. Soc. Jpn., 116 (2008), pp. 431-435, 10.2109/jcersj2.116.431
CrossRef Google Scholar

[34] E. Rudy
Ternary phase equilibria in transition metal-boron-carbon-silicon systems. Part 5. Compendium of phase diagram data
Rep. AFML TR-65-2 (1969), p. 732
View Record in Scopus Google Scholar

[35] L. Silvestroni, D.D. Fabbriche, D. Sciti
Tyranno SA3 fiber–ZrB_2 composites. Part I: microstructure and densification
Mater. Des., 65 (2015), pp. 1253-1263, 10.1016/j.matdes.2014.08.068
Article Download PDF View Record in Scopus Google Scholar